Chapter 7

Side Chain and Backbone Mutations Between Loops A and E of the $GABA_AR$ α_1 Subunit Alter Benzodiazepine Potentiation and GABA Activation

7.1 Introduction

γ-Aminobutyric acid type A ($GABA_A$) receptors are members of the Cys-loop family of ligand gated ion channels which mediate rapid synaptic transmission in the mammalian central nervous system. At rest the receptors are in a closed, non-conducting state. Upon binding of their cognate neurotransmitter agonist, the receptors undergo a conformational change, termed activation, to an open, ion-conducting state. Biochemical studies of these receptors has been guided by the X-ray crystal structure of the acetylcholine binding protein (AChBP)[1] and cryo-EM images of the *torpedo Californica* nicotinic acetylcholine receptor (nAChR).[2] Both these structures are highly homologous to nAChRs, another member of the Cys-loop family of receptors, and to a lesser extent other members of the superfamily. Homology models of the $GABA_AR$ based on both the AChBP and cryo-EM structures suggest the primary sequence linking loops A and E of the α_1 subunit of the $GABA_AR$ is highly unstructured (Figure 7.1).

In the preceding chapter, we identified this region of the receptor as a key element in the GABA activation pathway. Using photo-activated proteolytic cleavage of the $GABA_AR$ backbone (Chapter 6) we have shown that this linker must be intact for GABA activation and that the linker does not have a defined secondary structure in the closed state of the receptor. Proteolytic cleavage of the backbone introduces more flexibility to this region of the receptor and prevented GABA activation and therefore our ability to study the role of this region for benzodiazepine (BZD) potentiation. The added flexibility

in the primary structure may impact GABA activation directly or by displacing key amino acid side chains. In the present work we investigate these two affects separately.

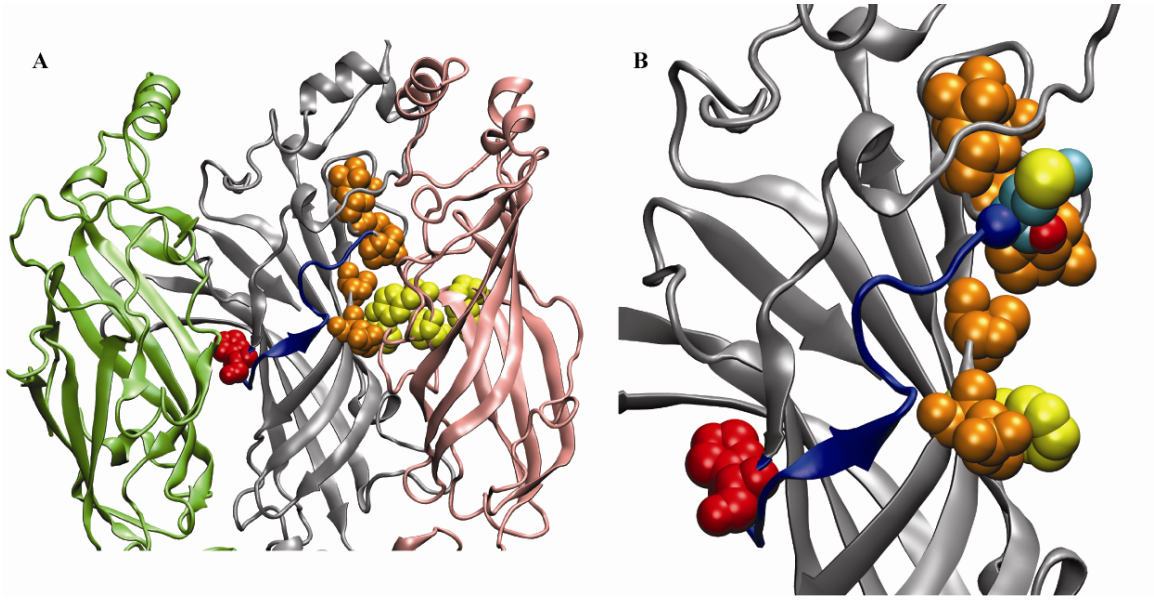

Figure 7.1 An unstructured linker connects loops A and E of the $GABA_AR$ α_1 subunit. **A,** the extracellular domain of three subunits, γ (lime), α (gray), and β (pink) as viewed from the channel pore. The loop A residue (red) and loop E residues (orange) of the α subunit are shown as Van der Waals residues. The GABA binding site is identified by yellow residues. **B,** The α subunit with the linker region (blue) highlighted. M113, the subject of the previous chapter, is shown in CPK coloring.

BZDs are allosteric modulators of the $GABA_AR$, and as such bind to the receptor at a site distinct from the GABA binding site. α_1His101, a loop A residue of the α_1 subunit, has been identified as contributing to the putative BZD binding site.[3-5] BZDs act in several ways including as inverse agonists inhibiting the GABA induced current,[6,7] positive modulators that potentiate the GABA current,[8] and antagonists that competitively bind at the BZD binding site but have no effect on GABA current.[9] The more common BZDs, flurazepam and diazepam, act by potentiating the GABA current, therefore application of these BZDs and GABA result in larger macroscopic current than application of GABA alone. Potentiation (P) is defined according to Equation 7.1

$$P = \frac{I_{FLZM}}{I_{GABA}} - 1 \qquad \textbf{Equation 7.1}$$

Given that the structural information[1,2] and available biochemical studies[10,*] indicate the region between loops A and E does not have a defined secondary structure, it is surprising that the primary sequences are highly conserved (Table 7.1). We noted no conserved differences in this region between the BZD sensitive (1-3, 5) and insensitive (4, 6) α subunits. We selected G103, K104, K105, M111, M113, and P114 for conventional mutagenesis. We reasoned that G103 and P114 present unique structural elements that may be crucial to receptor function. Conserved positive charges at K104 and K105 suggested a possible role for electrostatic interactions. M111 was selected because it is conserved as a hydrophobic residue but is only a Met in the α subunits. Finally, M113 was selected both due to less conservation and because it was previously used for Npg incorporation.

Table 7.1 Sequence Alignment of $GABA_AR$ subunits

GABA α_1	**P**	**D**	T	F	F	H	**N**	G	K	K	S	V	A	H	N	M	T	M	P	N	K	L	L	R	I
GABA α_2	**P**	**D**	T	F	F	H	**N**	G	K	K	S	V	A	H	N	M	T	M	P	N	K	L	L	R	I
GABA α_3	**P**	**D**	T	F	F	H	**N**	G	K	K	S	V	A	H	N	M	T	T	P	N	K	L	L	R	L
GABA α_4	**P**	**D**	T	F	F	R	**N**	G	K	K	S	V	S	H	N	M	T	A	P	N	K	L	F	R	I
GABA α_5	**P**	**D**	T	F	F	H	**N**	G	K	K	S	I	A	H	N	M	T	T	P	N	K	L	L	R	L
GABA α_6	**P**	**D**	T	F	F	R	**N**	G	K	K	S	I	A	H	N	M	T	T	P	N	K	L	F	R	I
GABA β_1	**P**	**D**	T	Y	F	L	**N**	D	K	K	S	F	V	H	G	V	T	V	K	N	R	M	I	R	L
GABA β_2	**P**	**D**	T	Y	F	L	**N**	D	K	K	S	F	V	H	G	V	T	V	K	N	R	M	I	R	L
GABA γ_1	**P**	**D**	T	F	F	R	**N**	S	R	K	S	D	A	H	W	I	T	T	P	N	R	L	L	R	I
GABA γ_2	**P**	**D**	T	F	F	R	**N**	S	K	K	A	D	A	H	W	I	T	T	P	N	R	M	L	R	I
GABA γ_3	**P**	**D**	T	I	F	R	**N**	S	K	T	A	E	A	H	W	I	T	T	P	N	Q	L	L	R	I
GABA γ_4	**P**	**D**	T	F	F	R	**N**	S	K	R	T	H	E	H	E	I	T	M	P	N	Q	M	V	R	I
						101												114							

The superfamily has a conserved WxPDxxxxN domain, the P, D, and N residues are shown in bold. Loop A residues are highlighted with red and loop E residues with yellow. G103, K104, K105, M111, M113, and P114 are colored as hydrophobic (red), polar (green), or cationic (blue).

[*] Chapter 6

Both glycine and proline are structurally unique when compared to the rest of the naturally occurring amino acids. Glycine (Figure 7.2) has a hydrogen atom as its side chain and therefore is not chiral. Its small size leads to fewer conformational restrictions and as such glycine residues are often found in hinge regions of proteins giving them a structural role in protein function.[11] Proline is the only naturally occurring cyclic amino acid and as such cannot make hydrogen bonds, as it lacks an N-H for hydrogen bonding. Additionally, proline can form *cis* amide bonds at a much higher frequency (~5%) than the other naturally occurring amino acids (<0.1%)[12] thus proline can also adopt unique conformations and often plays a structural role. For both glycine and proline residues, mutation to another naturally occurring amino acid often disrupts protein function,[13] and as such these residues seemed likely to play a role in activation.

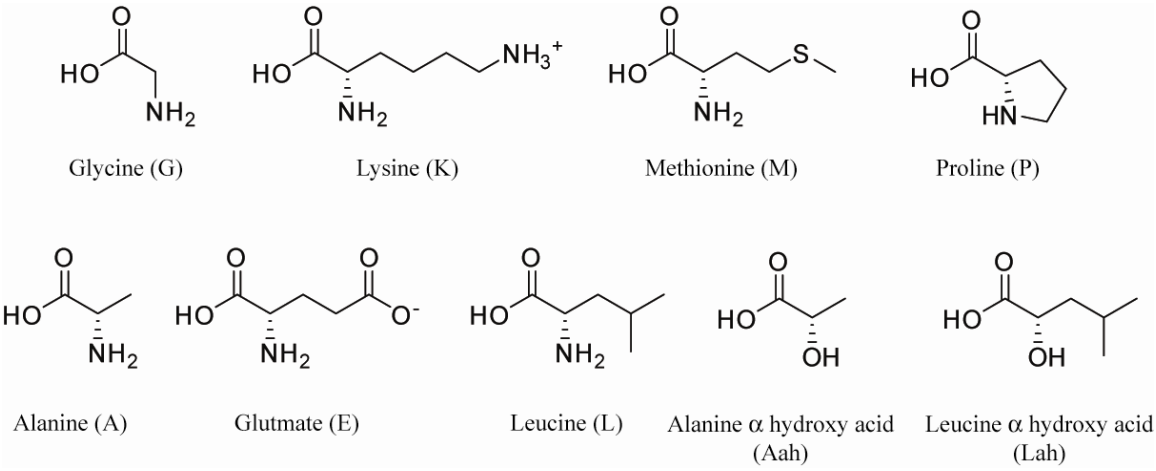

Figure 7.2 Chemical structures for wild type (top row) amino acids, conventional mutants (bottom row, left), and α-hydroxy acids (bottom, right)

7.2 Results

7.2.1 Conventional Mutagenesis – Side Chain Mutations

No electrical signal was detected for αG103Aβ $GABA_A$Rs even when the total mRNA was increased to 50 ng. The same mutation in the αβγ $GABA_A$R responded to

GABA in a concentration dependent manner. However, the amount of mRNA required was 100x greater than for wild type or other conventional mutants and I_{max} values were still lower than for most other mutations (Table 7.2). Despite lower current sizes, the GABA EC_{50} and Hill coefficient (n_H), as well as flurazepam (FLZM) potentiation (P) for αG103Aβγ $GABA_A$Rs were similar to wild type receptors. P114A mutant $GABA_A$Rs also behaved similarly to wild type receptors (Table 7.2). I_{max} values for the αP114Aβ $GABA_A$R were significantly lower than for wild type, but αP114Aβγ $GABA_A$R I_{max} values were similar to wild type. These data suggest that mutations in the αβ $GABA_A$R may affect surface expression to a greater extent than in the αβγ $GABA_A$R.

Table 7.2 Conventional mutagenesis in the linker region has little impact on EC_{50} (μM)

	$\alpha_1\beta_{2S}$ $GABA_A$R			**$\alpha_1\beta_{2S}\gamma_{2L}$ $GABA_A$R**			
Mutant	EC_{50}	n_H	I_{max}	EC_{50}	n_H	I_{max}	P
Wild type	1.8 ± 0.1	1.4	7 ± 1	44 ± 1	1.3	4.9 ± 0.6	2.6 ± 0.2
αG103A	NR			49 ± 4	1.4	1.4 ± 0.3	2.4 ± 0.8
αK104A	2.4 ± 0.2	1.1	3.6 ± 0.9	42 ± 3	1.1	2.4 ± 0.5	0.9 ± 0.1*
αK104E	5.9 ± 0.4	1.1	3.3 ± 0.6	64 ± 4	0.96	1.4 ± 0.2	2.2 ± 0.3
αK105A	8.4 ± 0.6	1.0	7 ± 1	87 ± 4	1.2	3.9 ± 0.9	1.5 ± 0.1*
αK105E	4.2 ± 0.1	1.2	5 ± 1	38 ± 2	1.5	11 ± 2	2.2 ± 0.2
αM111A	9.4 ± 0.7	0.93	3.7 ± 0.7	75 ± 3	1.0	2.4 ± 0.4	2.0 ± 0.2
αM111L	7.5 ± 0.4	1.1	4 ± 1	124 ± 6	1.1	2.1 ± 0.5	2.0 ± 0.2
αM113A	1.6 ± 0.1	1.4	7 ± 1	23 ± 1	1.3	9 ± 2	1.6 ± 0.2*
αM113L	4.7 ± 0.2	1.2	1.6 ± 0.2	73 ± 2	1.2	2.4 ± 0.6	1.2 ± 0.1*
αP114A	3.0 ± 0.1	1.2	2.3 ± 0.5	37 ± 2	1.3	3.5 ± 0.5	2.1 ± 0.3

NR denotes there was no response to 10 mM GABA. EC_{50} is reported in μM of GABA and I_{max} is reported in μA. All EC_{50} values are calculated from an average of at least 5 oocytes. Potentiation values are averaged from at least 8 oocytes, except for the G103A mutant which uses 4 oocytes. * indicates the potentiation is significantly different from wild type (two-tail unpaired t-test, $p<0.01$).

Amino acids at the positions analogous to K104 and K105 are conserved as positively charged amino acids in all the GABA α and β subunits. Given the proximity to the channel pore it seems reasonable that these side chains may stick into the channel pore and therefore may not interact with other side chains, rendering them insensitive to

mutation. However, these residues are conserved in the α_1, β_2, and γ_2 subunits, suggesting a positive ring of charge in this region of the receptor may be important. Surprisingly, removal of the side chain at αK104 (αK104A) had little effect on the EC_{50} of the αβ and αβγ $GABA_AR$ (Table 7.2), but a large effect on FLZM potentiation. The FLZM potentiation dropped to 0.9 (Figure 7.3) compared to 2.6 for the wild type receptor. The same mutation at position 105 (αK105A) increased EC_{50} for both αβ and αβγ receptors and decreased potentiation, though to a lesser extent than the αK104A mutation. Both alanine mutations had lower Hill coefficients than the wild type receptors, which may indicate a loss of cooperativity between subunits.

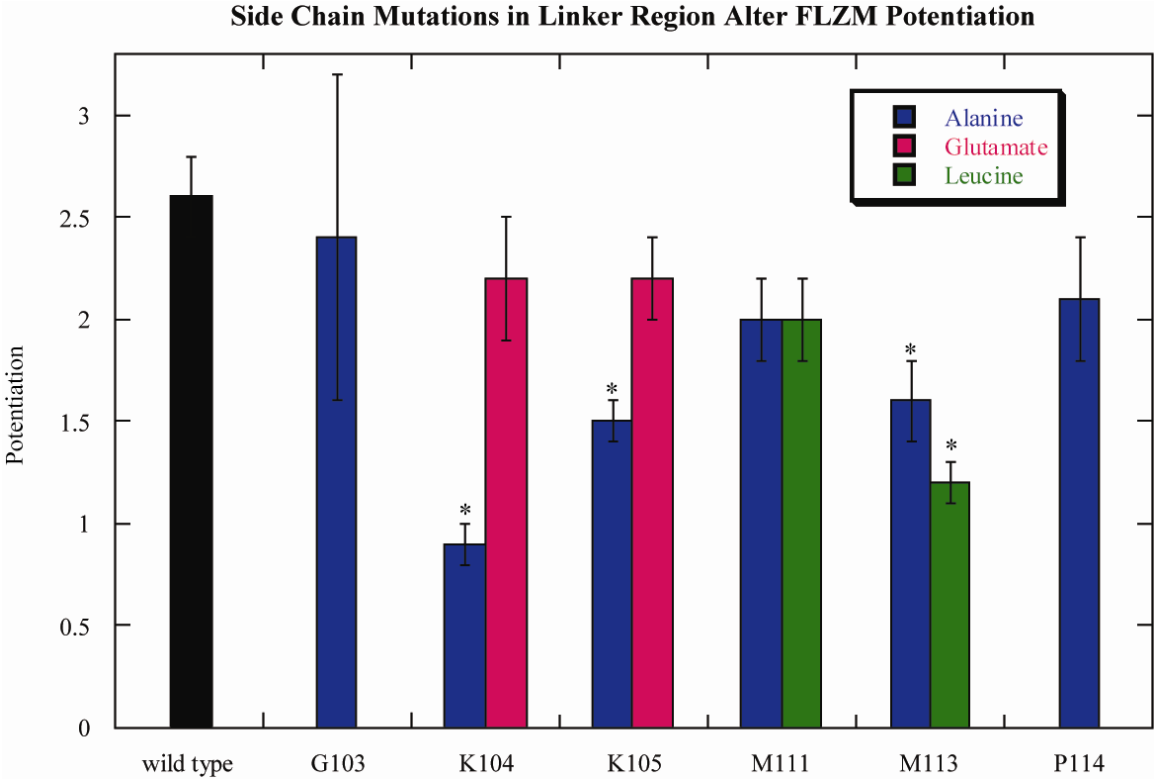

Figure 7.3 Conventional mutations in linker region alter FLZM potentiation. Four mutations, K104A, K105A, M113A, and M113L reduce FLZM potentiation. * indicates the value is significantly different from wild type (unpaired, two-tail t-test, $p<0.01$)

Charge reversal at positions 104 (αK104E) and 105 (αK105E) gave $GABA_A$Rs that functioned similarly to wild type receptors. The GABA EC_{50} of the αβ receptor increased ~3- and 2-fold, respectively. These mutations had a smaller impact on the GABA EC_{50} of the of the αβγ receptor such that values were not appreciably different form the wild type receptor. FLZM potentiation was not significantly different from wild type. Interestingly, the αK104E mutation lowered the Hill coefficient of both the αβ and αβγ receptors, indicating this residue may play a role in subunit cooperativity.

The methionine residues at positions 111 and 113 were mutated to alanine and leucine. αM111A and αM111L mutations increased the GABA EC_{50} 5.2- and 4.2-fold, respectively, in the αβ $GABA_A$R and 1.7- and 2.8-fold in the αβγ $GABA_A$R. Despite the shifts in GABA EC_{50}, neither mutation at αM111 altered FLZM potentiation. The opposite scenario occurred at αM113. For αM113 mutants, the GABA EC_{50} was not altered but FLZM potentiation decreased significantly. The αM113Aβ $GABA_A$R was nearly identical to the wild type receptor in terms of EC_{50}, Hill coefficient, and I_{max} values. In the αβγ receptor, this mutation was gain-of-function, lowering the EC_{50} ~2-fold. FLZM potentiation, however, was reduced to 1.6. The αM113L mutant, a more subtle mutation, increased EC_{50} slightly for both the αβ and αβγ $GABA_A$Rs yet decreased FLZM potentiation to only 1.2.

FLZM potentiation is dependent on the concentration of GABA and FLZM used. Potentiation is larger at lower concentrations of GABA (EC_{5-10}) thus we conducted all potentiation experiments within this range of GABA (Table 7.3). The FLZM concentration was held constant at 1 μM, which we initially assumed to be EC_{80-90} for all

mutations. To ensure this was the case, we determined the FLZM dose response relationship for the four mutations that altered FLZM potenitation as well as the M111A mutation (Table 7.3, Figure 7.4). The data indicate that 1 μM FLZM is between EC_{70-90} for all mutations and EC_{64} for the wild type receptor.

Table 7.3 The EC_{50} of potentiation ($EC_{50,P}$) and Hill coefficients for the FLZM dose response relationships

	$EC_{50,P}$ (nM)	n_H	$EC_{X,FLZM}$	N	[GABA]	$EC_{X,GABA}$
αβγ (WT)	500 ± 100	0.8 ± 0.1	64	12	5 μM	5.70
αK104Aβγ	220 ± 30	1.1 ± 0.1	84	5	5 μM	8.95
αK105Aβγ	300 ± 70	0.8 ± 0.1	72	4	10 μM	6.80
αM111Aβγ	300 ± 20	1.05 ± 0.06	78	5	5 μM	5.79
αM113Aβγ	400 ± 80	1.0 ± 0.1	71	5	3 μM	6.87
αM113Lβγ	230 ± 30	1.3 ± 0.2	87	4	10 μM	8.13

1 μM FLZM corresponds to EC_{64} for wild type and EC_{70-90} for all mutations. The concentration of GABA used for the potentiation and for determination of the FLZM dose response relationship was between EC_{5-10} for all mutations.

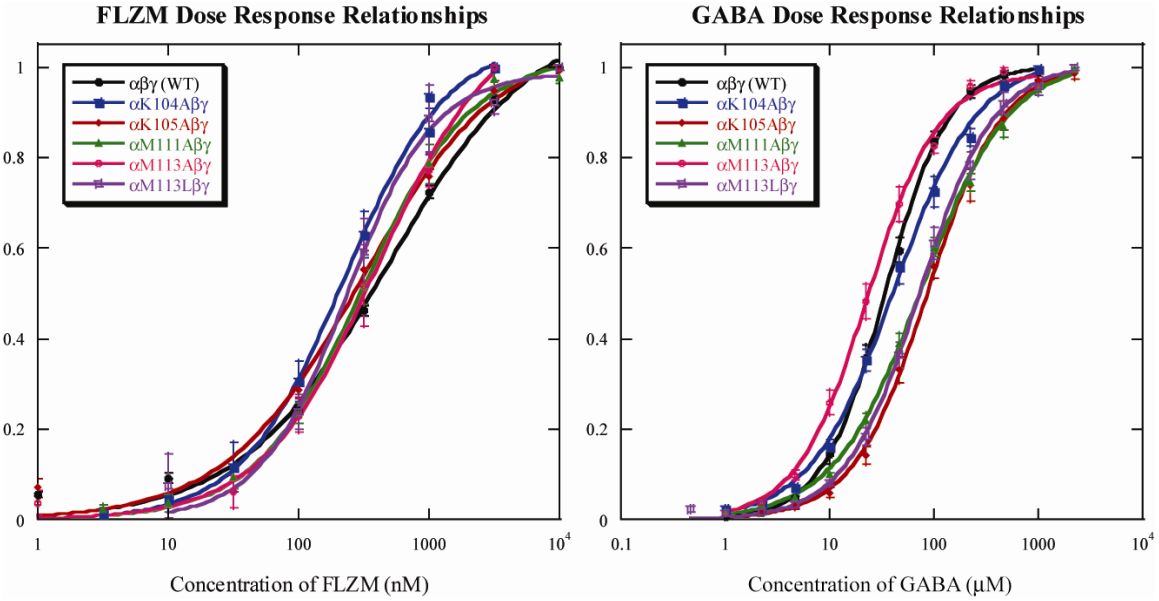

Figure 7.4 FLZM and GABA dose response relationships for wild type and selected conventional mutants. *Left*: Conventional mutations do not shift the FLZM dose response relationship significantly. *Right*: For comparison, the GABA dose response relationships are shown for the same mutations. There is more scatter in the GABA plot than the FLZM plot.

7.2.2 Incorporation of α-Hydroxy Acids

Side chain mutations at αM113 impacted FLZM potentiation while those at αM111 did not. Given the sensitivity of the region to proteolytic cleavage (Chapter 6), we reasoned that increasing the flexibility of the backbone, achieved by incorporation of an α-hydroxy acid, would either decrease potentiation with the αM111 mutations or rescue FLZM potentiation at αM113.

Table 7.4 Incorporation of α-hydroxy acids at αM111 increases GABA EC_{50} and decreases FLZM potentiation

Receptor	EC_{50} (μM)	n_H	I_{max} (μA)	P	ah/aa shift*
αM111Metβ	2.3 ± 0.1	1.3 ± 0.1	0.8 ± 0.2		
αM111Aahβ	120 ± 7	0.99 ± 0.05	1.0 ± 0.2		12.8
αM111Lahβ	31 ± 1	0.87 ± 0.02	2 ± 1		4.1
αM111(dCA)β			0.12 ± 0.05		
αM111Metβγ	41 ± 1	1.36 ± 0.05	3.5 ± 0.8	2.3 ± 0.2	
αM111Aahβγ	800 ± 40	0.97 ± 0.03	2.8 ± 0.4	0.54 ± 0.06	10.7
αM111Lahβγ	440 ± 30	0.90 ± 0.03	2.1 ± 0.2	1.3 ± 0.1	3.6
αM111(dCA)βγ	900 ± 100	0.81 ± 0.04	1.2 ± 0.1	0.67 ± 0.06	

*The final column gives the fold shift in GABA EC_{50} for the alpha hydroxy acid relative to the amino acid.

Incorporation of methionine by nonsense suppression at αM111 reproduced the GABA and FLZM behavior of the wild type αβ and αβγ wild type receptors (Table 7.4). Re-aminoacylation control (described in Chapter 6 and designated here as dCA) experiments gave maximal currents less than 150 nA in the αβ $GABA_AR$. The same experiments in the αβγ $GABA_AR$ gave significant current such that the GABA EC_{50} and Hill coefficient, as well as the FLZM potentiation, could be determined. Receptors resulting from re-aminoacylation of the suppressor tRNA and subsequent incorporation into the protein gave receptors with a pharmacology distinct from the wild type receptors. Incorporation of alanine-α-hydroxy acid (Aah, Figure 7.2) substantially increased the

EC_{50} (Table 7.4) of the αβ $GABA_AR$, as did leucine-α-hydroxy acid (Lah). Similar increases in GABA EC_{50} occurred for the αβγ $GABA_AR$ along with a decrease in FLZM potentiation. The GABA EC_{50} and Hill coefficient, as well as the FLZM potentiation for αM111Aahβγ $GABA_ARs$ is not pharmacologically different from the re-aminoacylation controls.

Wild type recovery (incorporation of methionine by nonsense suppression) experiments at αM113 yielded $GABA_ARs$ nearly identical to the wild type receptors for both the αβ and αβγ subtypes (Table 7.5). Re-aminoacylation control experiments gave enough current to determine the GABA EC_{50} and Hill coefficients in both subtypes as well as the FLZM potentiation in the αβγ receptor. These receptors were pharmacologically distinct from wild type. Aah increased the GABA EC_{50} slightly for both the αβ and αβγ receptors (Table 7.5). FLZM potentiation of the mutant receptor was similar to wild type. Incorporation of Lah substantially increased the EC_{50} of the αβ $GABA_AR$. The GABA EC_{50} of αM113Lahβγ $GABA_ARs$ is indistinguishable from that of the re-aminoacylation controls.

Table 7.5 Incorporation of α-hydroxy acids at αM113 increases GABA EC_{50} and decreases FLZM potentiation

Receptor	EC_{50} (μM)	n_H	I_{max} (μA)	P	ah/aa shift*
αM113Metβ	2.2 ± 0.1	1.5 ± 0.1	3.5 ± 1.1		
αM113Aahβ	3.7 ± 0.2	1.12 ± 0.07	0.9 ± 0.2		2.3
αM113Lahβ	26 ± 1	1.09 ± 0.04	1.5 ± 0.4		5.5
αM113(dCA)β	6.4 ± 0.8	0.77 ± 0.07	0.22 ± 0.07		
αM113Metβγ	43 ± 1	1.23 ± 0.04	4.5 ± 0.9	2.5 ± 0.2	
αM113Aahβγ	160 ± 20	0.84 ± 0.05	6 ± 2	2.8 ± 0.4	6.9
αM113Lahβγ	290 ± 20	1.05 ± 0.04	2.9 ± 0.5	1.45 ± 0.05	3.6
αM113(dCA)βγ	290 ± 40	0.92 ± 0.09	1.7 ± 0.4	0.81 ± 0.4	4.0

*The final column gives the fold shift in GABA EC_{50} for the alpha hydroxy acid relative to the amino acid.

7.3 Discussion

7.3.1 Side Chain Mutations: Affects on GABA EC_{50}

Conventional mutagenesis of the linker region had similar effects on GABA EC_{50} in both the αβ and αβγ $GABA_A$Rs, suggesting this region undergoes similar conformational changes during GABA activation in both receptor subtypes. The GABA EC_{50} shifts were generally larger in the αβ receptor, thus we restrict further discussion about the GABA EC_{50} to this subtype, unless otherwise specified. In the αβ $GABA_A$R, shifts in GABA EC_{50} for the alanine mutants ranged from 0.9 to 5.2-fold. Given the drastic nature of the alanine mutation, these shifts are relatively small, suggesting GABA activation is not highly dependent on side chain interactions with these residues. For the proposed structural residues, G103 and P114, we anticipated a much larger shift in the GABA EC_{50}, thus the data indicate that these two residues are not critical to the GABA activation pathway.

No electrical signal was detected for αG103Aβ mutant $GABA_A$Rs, suggesting the receptors could be non-functional or are not surface expressed. An inability for GABA to bind or disruption of the GABA activation pathway would both lead to non-functional receptors. αG103 is well removed from the GABA binding site, thus it seems unlikely that this mutation affects GABA binding. αG103Aβγ $GABA_A$Rs were surface expressed in sufficient quantity to determine the EC_{50} only when the amount of mRNA was increased 100-fold compared to the other conventional mutations. Given that increased mRNA amounts resulted in functional receptors with pharmacology similar to wild type and the location of αG103 near the subunit interface, it is most likely that αG103 plays a role in $GABA_A$R assembly and/or trafficking and thus that insufficient surface expression

of αG103Aβ $GABA_AR$ rather than nonfunctional receptors results in no detectable signal.

Charge reversal mutations at αK104 and αK105 are well tolerated. If these residues are involved in critical electrostatic interactions, we would expect mutation to alanine or glutamate to disrupt the interaction and severely impair channel function. Instead we see small shifts in EC_{50} (<5-fold), suggesting the residues are not involved in electrostatic interactions. Additionally, at αK105, charge reversal partially rescues the alanine mutation, suggesting an ionized species at this position aids channel function. At αK104, however, mutation to glutamate increased EC_{50} while alanine was similar to wild type. Taken together, the different results at these two positively charged, adjacent residues suggest the side chains are in distinct environments.

αM111 was most sensitive to side chain mutation. The alanine mutation produced the largest increase in EC_{50} (5.2-fold) of all the conventional mutations, indicating the methionine side chain may be important to receptor function. Interestingly, the more subtle mutation to leucine also increased EC_{50}. Like methionine, the leucine side chain is hydrophobic and relatively bulky (Figure 7.2). Chief structural differences between the two residues include a sulfur atom, one methylene difference in length, and branching in the leucine side chain. In contrast, αM113 was most tolerant of side chain mutations with mutation to alanine giving an EC_{50} nearly identical to wild type. Surprisingly, mutation to leucine, increased the EC_{50} (2.6-fold) slightly. This increase is only significant since alanine did not affect EC_{50}. At both methionine sites, mutation to leucine gives a larger increase in EC_{50} than expected for the subtlety of the mutation, especially given the data for the alanine mutations. These data strongly suggest the

GABA activation pathway is sensitive to the steric dimensions of the methionine side chains, such that introducing a γ-branched amino acid is sufficient to disrupt normal channel function.

7.3.2 Side Chain Mutations: Affects on FLZM Potentiation

Recent work by Kloda et al.[10] demonstrated that residues on loop E of the α subunit move when FLZM is applied to oocytes expressing mutant αβγ $GABA_AR$. The primary sequence of the α subunit links the BZD binding site (loop A) to loop E, thus it seems likely that residues in the linker would affect FLZM potentiation. Given that the linker is unstructured, we anticipated that side chain mutations would be unlikely to alter BZD potentiation. Initial experiments at two structural residues, G103 and P114, met our expectations, as the alanine mutants responded to FLZM similarly to wild type receptors. SCAM studies of these residues indicate that GABA and FLZM binding and activation are not affected by introduction of a larger MTSEA-Biotin group at G103[14] and P114.[10] The data from our studies corroborate the SCAM studies indicating the side chains of G103 and P114 are not integral to the mechanism of BZD potentiation.

At both αK104 and αK105, mutation to alanine decreased FLZM potentiation, clearly indicating the presence of a side chain is important to the potentiation mechanism. However, mutation to glutamate (present study) did not alter FLZM potentiation and mutation to cysteine did not alter FLZM EC_{50}.[14] Clearly, both cysteine and glutamate mutations are able to rescue the deleterious affect of mutation to alanine. SCAM studies of the cysteine mutation[14] indicate the side chain is either not accessible to MTSEA-biotin modification or that the modification does not affect GABA currents or FLZM

potentiation. Given that mutation to alanine caused decreased potentiation, but that cysteine, glutamate, and possibly MTSEA-biotin are able to function at these locations, it seems most likely that the size of both the K104 and K105 side chains is critical to FLZM potentiation.

Both αM113Aβγ and αM113Lβγ $GABA_A$Rs showed reduced FLZM potentiation, clearly indicating the side chain at this site is important to the potentiation mechanism. SCAM studies at this site indicate mutation to cysteine has a small effect on GABA EC_{50} and that MTSEA-biotin modification of the cysteine has a relatively small affect (~30% decrease) on GABA currents,[10] indicating the residue does not contribute to GABA binding and that side chain modifications do not prevent GABA activation. The SCAM study did not address FLZM induced changes at αM113. Our results, combined with the SCAM evidence showing αM113 modification does not impact GABA events, suggest that the side chain mutations affect only BZD potentiation. Interestingly, the same mutations at αM111 did not affect BZD potentiation, indicating the result is specific to αM113.

FLZM potentiation from application of 1 μM FLZM would be altered by changes to the potentiation pathway or by shifting the FLZM dose response curve. To ensure the dose response relationship was not altered, the potentiation dose response relationship was determined for representative mutations at each of K104, K105, M111, and M113. The data indicate that 1 μM FLZM is higher on the dose response curve for the mutant $GABA_A$Rs than for the wild type receptors; therefore if the FLZM potentiation pathway is unaffected by the mutations, we would expect wild type or higher potentiation values

in response to 1 μM FLZM. Thus, we can attribute the changes in FLZM potentiation from the conventional mutants to alterations of the potentiation mechanism.

It is interesting to note that, in several instances, mutations with small changes in GABA EC_{50} affected FLZM potentiation, while mutations with larger changes in GABA EC_{50} did not. αK104A $GABA_A$Rs had a smaller affect on GABA EC_{50} than αK104E $GABA_A$Rs, yet only the αK104A mutation affected FLZM potentiation. Similarly, mutations to αM111 had a larger impact on GABA EC_{50} than mutations to αM113, but FLZM potentiation was unaffected by αM111 mutant receptors and affected greatly by αM113 mutants. The trend is not perfect, as αG103A and αP114A receptors had small shifts in GABA EC_{50} and FLZM potentiation was unaffected, while at αK105 the alanine mutation had a larger effect on GABA EC_{50} and FLZM potentiation than the glutamate mutation. Still, if GABA activation and FLZM potentiation act through the same pathway, we would expect mutations to adversely impact both GABA EC_{50} and FLZM potentiation, which is clearly not always the case. The data presented herein indicate that while mechanisms of GABA activation and FLZM potentiation may be complementary[10,15,16] they clearly are not identical in terms of the involvement of amino acid side chains.

7.3.3 Backbone Mutations: Affects on $GABA_AR$ Activation

While we anticipated that α-hydroxy acid incorporation would alter receptor function, we were unsure if it would impact GABA EC_{50}, FLZM potentiation, or both, as well as whether the alteration would be a gain-of-function or loss-of-function. Additionally the α-hydroxy acids available were Aah and Lah, thus we wanted to be able to compare the affects of these mutations to that of the conventional mutant. Affects on

GABA EC_{50} and FLZM potentiation were similar for the alanine and leucine mutations at both αM111 and αM113, thus each of these sites already had an established pattern for the side chain mutations. Furthermore the established patterns for FLZM potentiation were opposite at the two sites, providing a means of detecting both gain-of-function or loss-of-function for the α-hydroxy acids.

The nonsense suppression methodology[17,18] is not perfect. In two cases presented here (αM111Aahβγ and αM113Lahβγ), we are unable to distinguish the data from α-hydroxy acid incorporation from that of the re-aminoacylation control experiment. We do note that in both cases the α-hydroxy acid experiments had approximately twice the current size of the controls and that the anticipated EC_{50} was similar to the measured EC_{50}. However, these results are not sufficient to definitively characterize the mutant receptor as distinct from the control experiments. Therefore, the remainder of the discussion and all conclusions drawn will not take into consideration the results from these two mutant receptors.

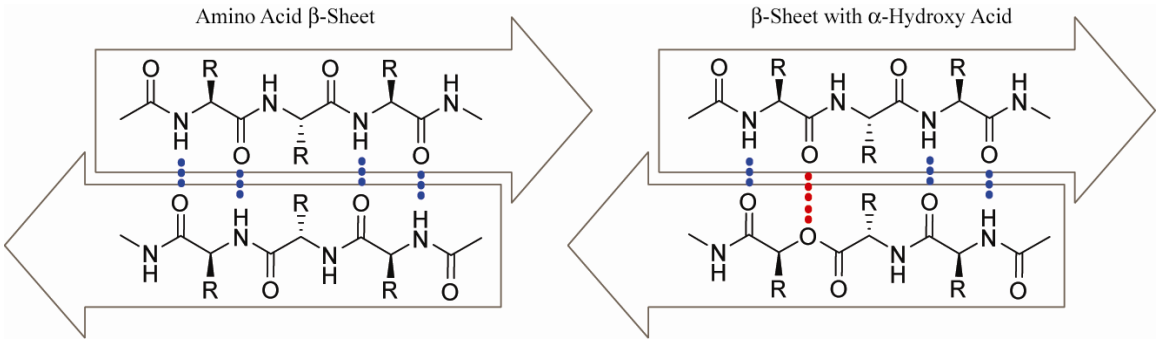

Figure 7.5 Hydroxy acids destabilize β-sheet structure. Typical β-sheets (left) have stabilizing (blue) hydrogen bond interactions between β-strands. When a α-hydroxy acid is incorporated (right) the attractive, stabilizing hydrogen bond interaction is replaced by a repulsive (red) O-O interaction, thereby destabilizing the secondary structure.

Incorporation of α-hydroxy acids at both positions increased the GABA EC_{50}. The changes were larger for αM111. Interestingly, Lah incorporation at both sites resulted in similar GABA EC_{50} values. These data clearly indicate that replacement of the amide bond with an ester bond impairs channel function, suggesting the region may adopt a defined secondary structure upon GABA activation. An increase in EC_{50} can be attributed to impaired GABA binding, stabilization of the closed state, destabilization of the open state or a combination of these factors. Given the location of the residues and previous biochemical studies,[10] it seems unlikely that backbone mutations will significantly impact GABA binding events. The structural information available indicates the region does not have a defined secondary structure (Figure 7.1)[1,2] and it is unlikely there are critical backbone interactions at both αM111 and αM113 that are not part of a secondary structure. However, the structural data is of the closed state of the receptor,[2] thus we cannot omit the possibility that this region adopts a β-strand configuration upon channel activation. If this is the case, α-hydroxy acid incorporation will de-stabilize the secondary structure because stabilizing hydrogen bonding interactions (Figure 7.5) have been deleted. Since the secondary structure is only present in the open state, these mutations will selectively de-stabilize the open state resulting in an increase in GABA EC_{50}. Furthermore, for a β-strand configuration we expect similar α-hydroxy acid incorporation at alternating residues to have similar affects, as seen here.

In addition to removing a potential hydrogen bond donating group, incorporation of α-hydroxy acids replaces an amide bond with a more flexible ester bond. We anticipated the added flexibility would either rescue FLZM potentiation at αM113 or impair FLZM potentiation at αM111. The data indicate that the added flexibility can

both impair and repair the potentiation pathway. Although this result is surprising, a straightforward interpretation exists: αM111 and αM113 undergo different changes during FLZM potentiation. The general activation pathways for GABA and BZD are anticipated to be similar, thus it is not surprising that αM111Lahβγ which has a large increase in GABA EC_{50} also has a decrease in FLZM potentiation, while αM113Aahβγ, which has a much smaller increase in GABA EC_{50}, has little affect on FLZM potentiation. Taken together, the α-hydroxy acid data indicate that GABA and FLZM induce similar structural rearrangements of the backbone within the linker region.

7.4 Conclusions

In conclusion, both side chain and backbone mutations between loops A and E of the α subunit affect GABA and FLZM activation pathways of the $GABA_AR$. Side chain mutagenesis, which is potentially more structurally perturbing, has a smaller affect on GABA EC_{50} than the more subtle mutation to a α-hydroxy acid, suggesting structural rearrangements of the entire linker are more critical than a particular side chain interaction. Furthermore, side chain mutations did not give consistent trends between changes in GABA EC_{50} and FLZM potentiation as expected, while backbone mutations both impaired GABA activation and decreased FLZM potentiation. The structural rearrangements within the linker likely initiate from loop E when GABA is applied and from Loop A when BZDs are applied. Thus it is possible that the final state of the backbone is similar for both activation pathways while the nature and sequence of the conformational changes are not. Different conformational changes to arrive in the same final state would allow for different affects on GABA EC_{50} and FLZM potentiation for side chain mutations, while still accounting for the similar affects for the backbone

mutations. Overall the data support a structural rearrangement of the primary sequence between loops A and E of the α subunit during GABA activation and FLZM potentiation.

7.5 Materials and Methods

Mutagenesis and preparation of mRNA: Human α_1 and β_{2S} $GABA_AR$ genes in pGEMHE were obtained from S.C.R. Lummis (Department of Biochemistry, University of Cambridge, Cambridge, United Kingdom). Quickchange PCR was used to make α_1 mutant DNA and mutation was confirmed by sequencing (Laragen Sequencing). The cDNA was linearized using Nhe1 (Roche) for the α_1 subunit and either Spe1 (Roche) or Sph1 (Roche) for the β_{2S} subunit. The mMessage mMachine kit (Ambion) was used to generate capped mRNA for oocyte injection.

7.5.1 Oocyte Injection

$\alpha\beta$ $GABA_AR$: For wild type and conventional mutations $\alpha_1\beta_{2S}$ mRNA was mixed in a 1:1 ratio and diluted to a final concentration of 100 ng/μl unless otherwise noted. Each oocyte was injected with 50 nl (5 ng) of mRNA mix. For suppression experiments, a 5:1 mix of the mRNA of the mutated α_1 gene and β_{2S} at a final concentration of 1 μg/μl was used.

$\alpha\beta\gamma$ $GABA_AR$: For wild type and conventional mutations, the β_{2S} gene was linearized with Spe1 and a 2:2:1 ratio of α:β:γ diluted to a final concentration of 10 ng/μl (unless otherwise noted) was used for mRNA mix as this yielded a pure population of αβγ receptors (see Appendix for additional details) with I_{max}values between 1 and 10 μA. For suppression experiments, the β_{2S} gene was linearized with Sph1 and a 5:1:5 ratio of α:β:γ at a final concentration of 1 μg/μl was used for the mRNA mix.

Suppression experiments: The mRNA mix was mixed 1:1 (by volume) with the deprotected aa-tRNA or ah-tRNA ($tRNA_{CUA}$ charged with either a naturally occurring amino acid or a α-hydroxy acid). Each oocyte was injected with a total volume of 50 nl of RNA mix; 25 ng mRNA and 15-50 ng of aa-tRNA (or ah-tRNA). The aa-tRNA was stored with the amino group protected by an NVOC group. Prior to mixing the aa-tRNA with the mRNA mix, the aa-tRNA was deprotected by photolysis. α-Hydroxy acids are not stored with a protecting group.

Met-, Aah- and Lah-tRNA were prepared as described previously.[17-19] Briefly, Met was protected using a nitroveratryloxycarbonyl group. The carboxylic acid of Met-NVOC, Aah and Lah were activated as the cyanomethyl esters and the activated compound was coupled to the dinucleotide dCA, which was then enzymatically ligated to 74-mer THG73 $tRNA_{CUA}$.

7.5.2 Characterization of Mutant Receptors

After injection, oocytes were incubated for 24-48 hours at 18°C prior to electrophysiology recordings. For a control, cRNA alone and cRNA mixed with dCA-THG (no unnatural amino acid attached) were injected into oocytes.

Determination of GABA EC_{50}: Peak GABA-induced currents were recorded at 19-22°C from individual oocytes using the OpusXpress system (Axon Instruments, Molecular Devices). A stock solution of 10 mM GABA (Sigma, St. Louis, MO) in ND96 buffer (in mM: 96 NaCl, 2 KCl, 1 MgCl2, 1.8 CaCl2, 5 HEPES, pH 7.5) was made fresh for each recording session. Drug solutions were made from the stock by dilution in ND96 buffer. Drug was delivered to cells via the automated perfusion system of the OpusXpress. Glass microelectrodes were backfilled with 3 M KCl and had a resistance

of 0.5-3.0 MΩ. The holding potential was -60 mV. To determine EC_{50} values, GABA concentration-response data were fitted to the Hill equation (Equation 7.2), where I_{max} is the maximal peak current and n is the Hill coefficient.

$$I = \frac{I_{\max}}{1 + EC_{50}/[A]^n} \qquad \textbf{Equation 7.2}$$

Flurazepam Potentiation: Potentiation was determined using $EC_{5\text{-}10}$ of GABA. A high dose of GABA (>EC_{50}) was applied for 30 seconds then washed out (315 seconds between drug applications) and followed by $EC_{5\text{-}10}$ GABA applied three times (315 seconds between doses). A final drug application of 1 μM FLZM and $EC_{5\text{-}10}$ GABA was then applied. The average I_{max} of the three GABA applications was calculated and is represented by I_{GABA} in Equation 7.2. The peak of the potentiated current (I_{FLZM}) is the peak current due to application of both FLZM and GABA. Potentiation (P) was calculated according to Equation 7.1. Only oocytes with a standard error < 10% of I_{GABA} were considered to have stable currents. Only oocytes with stable GABA currents were used to determine potentiation.

Determination of Flurazepam EC_{50} ($EC_{50,P}$): For these experiments, the total concentration of mRNA used for oocyte injection was increased to 100 ng/μl to increase current size. The EC_{50} of potentiation, $EC_{50,P}$, was determined with a background GABA concentration of $EC_{5\text{-}10}$. FLZM was added in increasing concentrations (stating with 0 μM) until maximal potentiation was achieved. The data were fit to the Hill equation (Equation 7.1) to obtain the $EC_{50,P}$ and Hill coefficients. For each dose, oocytes were washed with ND96 for 30 seconds, followed by ND96+GABA ($EC_{5\text{-}10}$) for 30 seconds, then 1 mL of FLZM+GABA was applied over 30 seconds, followed by a 285 second

wash with ND96. The peak current was calculated by measuring the peak of the FLZM+GABA current and subtracting out the GABA only current immediately prior to application of FLZM+GABA.

7.6 References

(1) Brejc, K.; van Dijk, W. J.; Klaassen, R. V.; Schuurmans, M.; van Der Oost, J.; Smit, A. B.; Sixma, T. K. *Nature* **2001**, *411*, 269-76.
(2) Unwin, N. *J Mol Biol* **2005**, *346*, 967-89.
(3) Berezhnoy, D.; Nyfeler, Y.; Gonthier, A.; Schwob, H.; Goeldner, M.; Sigel, E. *J Biol Chem* **2004**, *279*, 3160-8.
(4) Buhr, A.; Baur, R.; Malherbe, P.; Sigel, E. *Mol Pharmacol* **1996**, *49*, 1080-4.
(5) Kucken, A. M.; Teissere, J. A.; Seffinga-Clark, J.; Wagner, D. A.; Czajkowski, C. *Mol Pharmacol* **2003**, *63*, 289-96.
(6) Oakley, N. R.; Jones, B. J. *Neuropharmacology* **1982**, *21*, 587-9.
(7) Macdonald, R. L.; Twyman, R. E.; Ryan-Jastrow, T.; Angelotti, T. P. *Epilepsy Res Suppl* **1992**, *9*, 265-77.
(8) Macdonald, R.; Barker, J. L. *Nature* **1978**, *271*, 563-4.
(9) Braestrup, C.; Schmiechen, R.; Neef, G.; Nielsen, M.; Petersen, E. N. *Science* **1982**, *216*, 1241-3.
(10) Kloda, J. H.; Czajkowski, C. *Mol Pharmacol* **2007**, *71*, 483-93.
(11) Fasman, G. D. *Prediction of protein structure and the principles of protein conformation*; Springer, **1989**.
(12) Jabs, A.; Weiss, M. S.; Hilgenfeld, R. *J Mol Biol* **1999**, *286*, 291-304.
(13) Lee, W. Y.; Sine, S. M. *Nature* **2005**, *438*, 243-7.
(14) Sharkey, L. M.; Czajkowski, C. *Mol Pharmacol* **2008**, *74*, 203-12.
(15) Changeux, J. P.; Edelstein, S. J. *Neuron* **1998**, *21*, 959-80.
(16) Olsen, R. W. *Annu Rev Pharmacol Toxicol* **1982**, *22*, 245-77.
(17) Nowak, M. W.; Gallivan, J. P.; Silverman, S. K.; Labarca, C. G.; Dougherty, D. A.; Lester, H. A. *Methods Enzymol* **1998**, *293*, 504-29.
(18) Nowak, M. W.; Kearney, P. C.; Sampson, J. R.; Saks, M. E.; Labarca, C. G.; Silverman, S. K.; Zhong, W.; Thorson, J. S.; Abelson, J. N.; Davidson, N.; Schultz, P. G.; Dougherty, D. A.; Lester, H. A. *Science* **1995**, *268*, 439-442.
(19) England, P. M.; Lester, H. A.; Davidson, N.; Dougherty, D. A. *Proc Natl Acad Sci U S A* **1997**, *94*, 11025-30.